Int. J. Electrochem. Sci., 9 **(2014)** 5585 - 5595

International Journal of ELECTROCHEMICAL SCIENCE
www.electrochemsci.org

Relevance of Electrochemical and Surface Studies to Probe *Zanthoxylum schinifolium* (sichuan pepper) as an Effective Corrosion Inhibitor for N80 steel in CO_2 Saturated 3.5% NaCl Solution

Ambrish Singh[1,2], *Yuanhua Lin*[1,*], *Eno. E. Ebenso*[3,4], *Wanying Liu*[1], *Deng Kuanhai*[5], *Jie Pan*[5], *Bo Huang*[5]

[1] State Key Laboratory of Oil and Gas Reservoir Geology and Exploitation, Southwest Petroleum University, Chengdu, Sichuan 610500, China.
[2] Department of Chemistry, School of Civil Engineering, LFTS, Lovely Professional University, Phagwara, Punjab, India.
[3] Department of Chemistry, School of Mathematical & Physical Sciences, North-West University(Mafikeng Campus), Private Bag X2046, Mmabatho 2735, South Africa.
[4]Material Science Innovation & Modelling (MaSIM) Focus Area, Faculty of Agriculture, Science and Technology, North-West University (Mafikeng Campus), Private Bag X2046, Mmabatho 2735, South Africa.
[5]CNPC Key Lab for Tubular Goods Engineering (Southwest Petroleum University), Chengdu, Sichuan 610500, China.
[*]E-mail: yhlin28@163.com

Received: 21 February 2014 / *Accepted:* 17 May 2014 / *Published:* 16 July 2014

The inhibition of the corrosion of N80 steel in 3.5 wt.% NaCl solution saturated with CO_2 by the extract of *Zanthoxylum schinifolium* (ZSE) has been studied using electrochemical impedance spectroscopy (EIS), potentiodynamic polarization, X-ray diffraction (XRD) and scanning electron microscopy (SEM). Inhibition efficiency was found to increase with increasing concentration of the extract. The adsorption of the extract on the N80 steel surface obeyed the Temkin adsorption isotherm. Values of inhibition efficiency calculated from potentiodynamic polarization, and electrochemical impedance spectroscopy (EIS) are in good agreement. Polarization curves showed that ZSE behaves as a mixed-type inhibitor in NaCl solution. The adsorbed film on N80 steel surface containing inhibitor was confirmed by the XRD, SEM results. The results obtained showed that the ZSE could serve as an effective inhibitor of the corrosion of N80 steel in 3.5% NaCl saturated with CO_2.

Keywords: *Zanthoxylum schinifolium*; N80 steel; Corrosion inhibitor; EIS; XRD; SEM

1. INTRODUCTION

Metals and alloys used in many oil wells are susceptible to corrosion in aqueous media. N80 steel, the most widely used among them, is also highly susceptible to corrosion, especially in aqueous media [1]. N80 steel is widely used as a construction material for pipe work in the oil and gas production, such as downhole tubular, flow lines, and transmission pipelines in the petroleum industry. Aqueous carbon dioxide (carbonic acid) is corrosive and corrodes the carbon steel pipelines. Carbon dioxide corrosion has been of interest to researchers in oil industries for many years and there exists many theories about the mechanism of CO_2 corrosion [2].

Therefore, protective measures should be required to prevent the metal loss due to corrosion by using chemical and other means. One of the best known methods for corrosion protection is the use of inhibitors as no special equipments required, low cost and easy operation. It is highly desired that new inhibitors for N80 steel are non-toxic and environment-friendly. Most of the well-known inhibitors are organic compounds containing nitrogen, oxygen, and/or sulfur atoms; heterocyclic compounds; and delocalized π-electrons. It is generally accepted that organic molecules inhibit corrosion via adsorption at the metal solution interface [3-6], making the adsorption layer to function as a barrier and isolating the metal from the corrosion [7, 8].

Zanthoxylum schinifolium found in China, Japan and Korea, is an aromatic shrub with protective thorns and culinary and pharmacological properties which has been cultivated in the southern provinces of China [9, 10]. Previous phytochemical studies indicated coumarins, alkaloids, triterpenoids, steroids, and flavonoids in the extract of ZSE [11, 12].

The present study investigates the inhibiting effect of *Zanthoxylum schinifolium* (ZSE). Inhibition effect of ZSE on the corrosion of N80 steel in CO_2 saturated 3.5% NaCl solution was studied by potentiodynamic polarization and electrochemical impedance spectroscopy (EIS) methods. Meanwhile, the steel surface was examined by scanning electrochemical microscopy (SECM), X-ray diffraction (XRD) and scanning electron microscopy (SEM) techniques.

2. EXPERIMENTAL

2.1. Preparation of inhibitor

Fifty grams of dried *Zanthoxylum schinifolium* (ZSE) were soaked in 900 ml of reagent grade ethanol for 24 h and refluxed for 5 h. The ethanolic solution was filtered and concentrated to 500 ml. This extract was used to study the corrosion inhibition properties.

2.2. Materials and Solutions

N80 steel having the following chemical composition (wt %): C 0.31; Si 0.19; Mn 0.92; P 0.010; S 0.008; Cr 0.2; Fe balance were used for all studies. N80 steel coupons having dimensions of 10 mm × 10 mm × 3 mm were used for the electrochemical study. The specimens were welded with

copper wire and covered with epoxy resin. The specimens were metallographically polished according to ASTM A262, degreased and dried before experiment. The test solution of 3.5% NaCl was prepared by analytical grade NaCl with double distilled water. All experiments were performed at room temperature and in unstirred solution.

2.3. Electrochemical measurements

The electrochemical experiments were performed by using three electrode cell, connected to Potentiostat/Galvanostat AUTOLAB model GSTAT302N. Autolab applications include software FRC and GPES for corrosion and EIS measurements and data fitting. N80 steel was used as working electrode, platinum electrode as an auxiliary electrode, and saturated calomel electrode (SCE) as reference electrode. All potentials reported were measured versus SCE. Tafel curves were obtained at a scan rate of 1.0 mVs^{-1}. EIS measurements were performed under potentiostatic conditions in a frequency range from 100 kHz to 0.01 Hz, with amplitude of 10 mV AC signal. The experiments were carried out when the electrochemical system was in steady state in 3.5% NaCl saturated with CO_2 in absence and presence of different concentrations of ZSE. Prior to the electrochemical measurement, a stabilization period was allowed to attain a stable value of E_{corr}.

2.4. X-Ray Diffraction (XRD)

The N80 steel specimens were immersed in CO_2 saturated 3.5% NaCl solution in absence and presence of inhibitor for a period of 3 hr. After then, the specimens were taken out and dried. The surface film formed on the surface of the mild steel specimen was analyzed by using X-ray diffractometer, X Pert PRO incorporated with Higscore software.

2.5. Scanning Electron Microscopy (SEM)

The electrodes were immersed in the test solution (CO_2 saturated 3.5% NaCl) in the absence and presence of corrosion inhibitor to observe the effect of corrosion and inhibition. The N80 steel electrodes were then dried at ambient temperature. Micrographs of abraded and corroded N80 steel surfaces and those after inhibitor addition were taken using a SEM model TESCAN VEGA II XMH instrument.

3. RESULTS AND DISCUSSION

3.1. Electrochemical measurements

3.1.1. Electrochemical Impedance Spectroscopy (EIS)

Impedance spectra for N80 steel in CO_2 saturated 3.5% NaCl in absence and presence of different concentrations of ZSE are shown in the form of Nyquist plots (figure 1a), Bode-modulus plots (figure 1b) and in the Theta-frequency format (figure 1c).

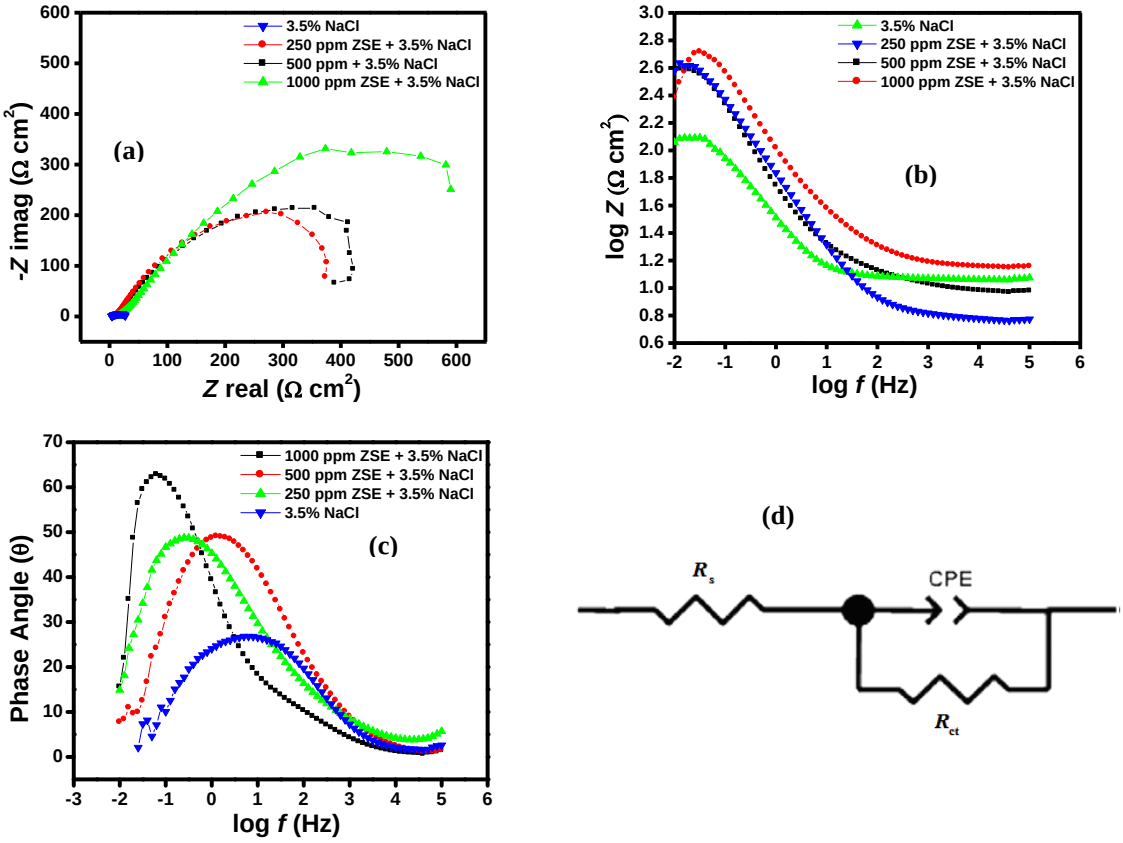

Figure 1. Electrochemical impedance plots for (a) Nyquist (b) Bode (c) Theta frequency and (d) equivalent circuit in absence and presence of ZSE for N80 steel.

Although the appearance of Nyquist plots remained the same, their diameter increased after the addition of ZSE to the corrosive solution. This increase was more and more pronounced with increasing inhibitor concentration indicating the adsorption of inhibitor molecules on the metal surface [13]. However, after the addition of ZSE, the impedance modulus of the system gradually increased and was a maximum in the case of ZSE at 1000 ppm. The impedance diagram (Nyquist) contains depressed curves with the center under the real axis with one capacitive loop in the high frequency (HF) zone. As usually indicated in an EIS study, the HF capacitive loop is related to the charge-transfer resistance process of the metal corrosion and the double-layer behavior, and these loops are not perfect semicircles. The charge transfer resistance increased with increase in concentration of inhibitor [14-18]. The curve in the Nyquist plot is depressed, which we attribute to surface roughness and the resulting distortion of the double layer.

The model used for fitting consist of R_s (the resistance of solution between working electrode and counter electrode), R_{ct}, and the constant phase angle element (CPE) as shown in figure 1d. The double layer usually behaves as a constant-phase element (CPE) rather than as a pure capacitor. The CPE is substituted for the capacitor to fit the curve more accurately. The capacitance values were calculated using the equation [17, 18]:

$$Z_{CPE} = Q^{-1}(j\omega)^{-n} \quad (1)$$

where Q is the magnitude of the CPE, j is the imaginary unit, ω is the angular frequency (ω = 2πf, the frequency in Hz), and n is the phase shift which can be used as a gauge of the heterogeneity and gives details about the degree of surface inhomogeneity (roughness). Depending on the value of n, *CPE* can represent resistance (n = 0, Q = R), capacitance (n = 1, Q = C), inductance (n = -1, Q = L) or Warburg impedance (n = 0.5, Q = W). In fact, when n is close to 1, the CPE resembles a capacitor, but the phase angle is not 90°. It is constant and somewhat less than 90° at all frequencies. The inhibition efficiency is calculated using charge transfer resistance (R_{ct}) as follows,

$$\eta\% = \frac{R_{ct(inh)} - R_{ct}}{R_{ct(inh)}} \times 100 \quad (2)$$

Where $R_{ct(inh)}$ and R_{ct} are the values of charge transfer resistance in presence and absence of inhibitor in 3.5% NaCl respectively. At different concentrations ZSE showed increase in value of R_{ct} with respect to blank 3.5% NaCl solution. The increase in R_{ct} values as shown in table 1 is attributed due to increase in resistance and adsorption of inhibitor molecules on N80 steel surface [19-22]. Also any significant change in the values of the phase shift, n, was not observed in the absence and in the presence of ZSE. To predict the dissolution mechanism, the value of n can be used as an indicator. The values of n, ranging between 0.829 and 0.878, indicate that the charge transfer process controls the dissolution mechanism of N80 steel in CO_2 saturated 3.5% NaCl solution in the absence and in the presence of ZSE

Table 1. Nyquist data for N80 steel in 3.5% NaCl at different concentration of ZSE.

Solutions	Conc.(ppm)	R_s (Ω cm^2)	R_{ct} (Ω cm^2)	η%	θ	n
3.5% NaCl	-	9.0	25	-	-	0.829
ZSE	250 ppm	9.6	373	93	0.93	0.867
ZSE	500 ppm	8.7	410	93	0.93	0.845
ZSE	1000 ppm	9.4	590	95	0.95	0.878

3.1.2. Potentiodynamic polarization measurements

Table 2. Tafel polarization data for N80 steel in 3.5% NaCl at different concentration of ZSE.

Solutions	Tafel data						
	Conc.(ppm)	E_{corr} (V vs. SCE)	I_{corr} (A cm^{-2})	b_a (V d^{-1})	b_c (V d^{-1})	η% (%)	θ
3.5% NaCl	-	-0.632	8.60	1.28	1.78	-	-
ZSE	250 ppm	-0.647	2.32	1.13	0.19	73	0.73
ZSE	500 ppm	-0.689	1.52	1.27	0.08	82	0.82
ZSE	1000 ppm	-0.619	0.51	0.09	0.44	94	0.94

Electrochemical kinetic parameters such as corrosion potential (E_{corr}), corrosion current density (I_{corr}), and anodic (β_a) and cathodic (β_C) slopes are obtained by the anodic and cathodic regions of the tafel plots shown in table 2.

The corrosion current density (I_{corr}) can be obtained by extrapolating the tafel lines to the corrosion potential and the inhibition efficiency (η %) values were calculated from the relation:

$$\eta\% = \frac{I_{corr} - I_{corr(i)}}{I_{corr}} \times 100 \quad (3)$$

Where, I_{corr} and $I_{corr(i)}$ are the corrosion current density in absence and presence of inhibitor. The polarization curves for N80 steel in the absence and presence of the inhibitor are given in figure 3.

The liberation of H^+ ions is reduced due to addition of the inhibitor. The inhibitor molecules are first adsorbed on the surface and blocked the active sites of the steel surface.

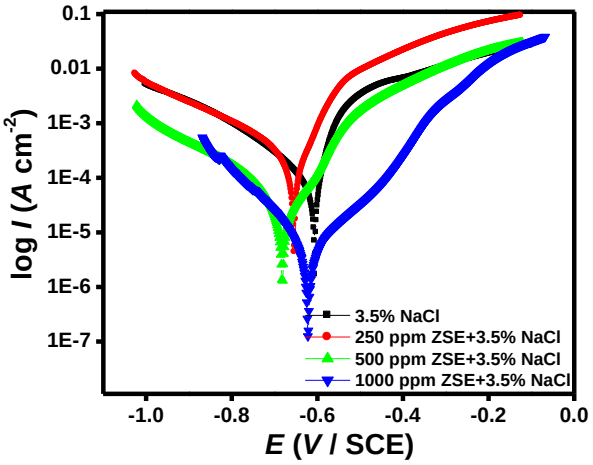

Figure 3. Tafel polarization plots for N80 steel in absence and presence of ZSE.

The values of b_a were shifted to higher values and b_c values shifted to lower values with reference to blank in the presence of ZSE. This showed that ZSE inhibits the corrosion process by controlling anodic and cathodic reactions predominantly of the metal surface [23]. I_{corr} values decreased with increase in concentration inhibitor. This result confirmed the inhibitive action of ZSE toward corrosion of the N80 steel.

But, analysis of both anodic (b_a) and cathodic (b_c) tafel slope values indicated that both anodic and cathodic reactions were suppressed during the addition of the inhibitor, which suggested that the ZSE reduced anodic dissolution and also retarded the hydrogen evolution reaction [24-26]. Since both the anodic and cathodic sites were suppressed therefore ZSE acted as a mixed type inhibitor.

3.2. Adsorption isotherm

Adsorption isotherms always play a vital role in determining mechanism of corrosion reactions. The adsorption of an organic adsorbate on to metal-solution interface can be represented by a

substitutional adsorption process between the organic molecules in the aqueous solution phase ($Org_{(sol)}$) and the water molecules on the metallic surface ($H_2O_{(ads)}$) [27].

$$Org_{(sol)} + xH_2O \rightarrow Org_{(ads)} + xH_2O_{(sol)} \quad (4)$$

where, x is the size ratio representing the number of water molecules replaced by one molecule of organic adsorbate.

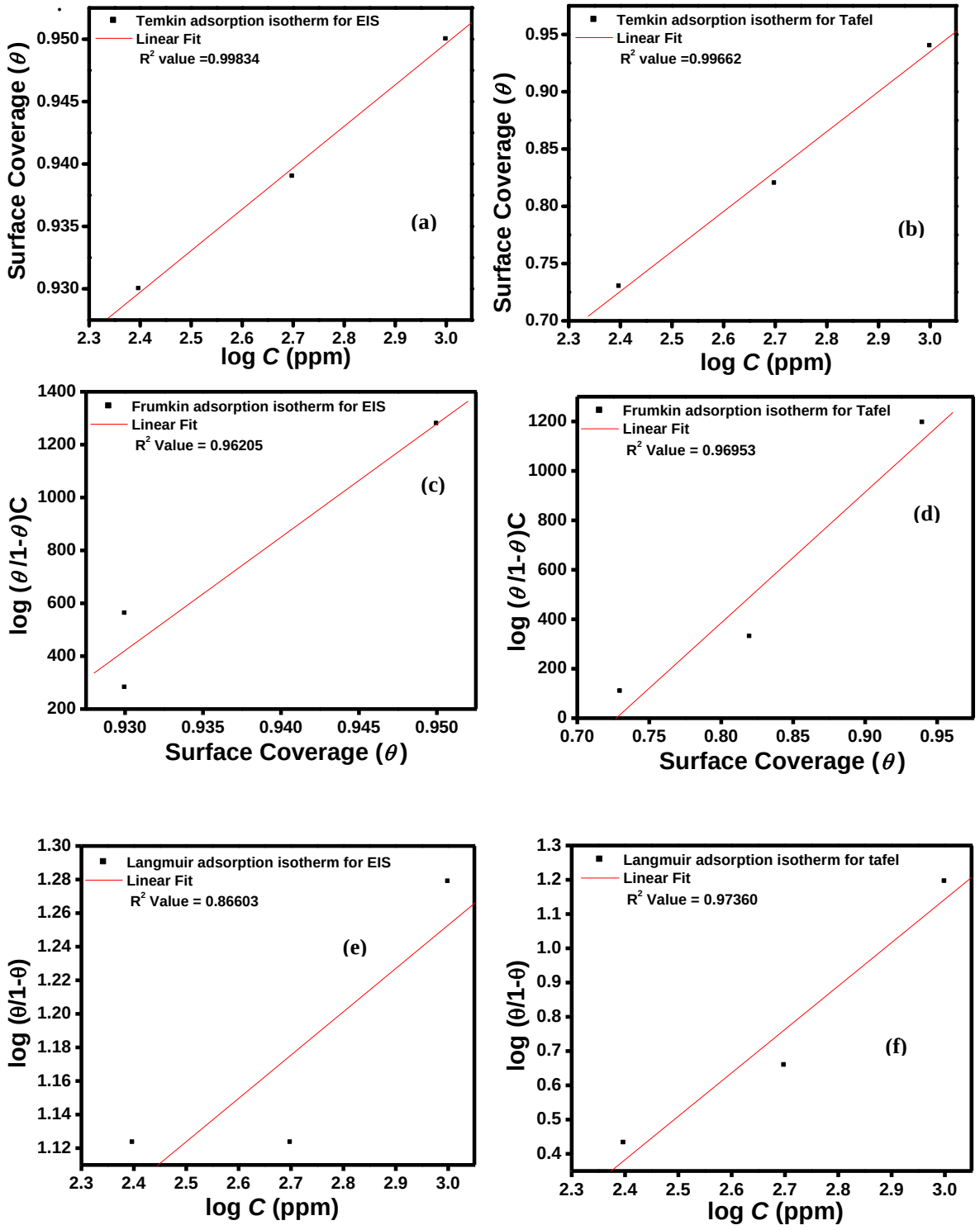

Figure 4. The adsorption isotherm plots for (a) Langmuir EIS (b) Langmuir Tafel (c) Frumkin EIS (d) Frumkin Tafel (e) Temkin EIS and (f) Temkin Tafel at different concentrations of ZSE.

Basic information on the interaction between the inhibitor and the N80 steel surface can be provided by the adsorption isotherm. It is essential to know the mode of adsorption and the adsorption isotherm that can give important information on the interaction of inhibitor and metal surface. Attempts were made to fit the θ values to various isotherm including Temkin (4a, b), Frumkin (4c, d) and Langmuir (4e, f). The plot of surface coverage (θ) as a function of logarithm of inhibitor concentration (log C) was evaluated. The correlation coefficients (R^2) were used to determine the best fits. Assumptions of Langmuir, Frumkin and Temkin were made according to the equations given below:

$$\theta = \frac{bC_{inh}}{1+bC_{inh}} \quad \text{(Langmuir Isotherm)} \quad (5)$$

$$\exp(-2a\theta) = K_{ads}C_{inh} \quad \text{(Temkin isotherm)} \quad (6)$$

$$K_{ads}C = \frac{\theta}{1-\theta}e^{f\theta} \quad \text{(Frumkin isotherm)} \quad (7)$$

where, b designates the adsorption coefficient in equation (5), a the molecular interaction parameter, θ is the surface coverage, C is the inhibitor concentration in equation (6, 7). By plotting values of log C versus values of surface coverage (θ), straight line graphs were obtained (Figure 4a, b), which suggested the adsorption of ZSE on metal surface obeyed Temkin adsorption isotherm. The obtained plots of the ZSE were almost linear with correlation coefficient (R^2) ranging 0.99834 for EIS (Figure 4a) and 0.99662 for Tafel polarization (Figure 4b). The straight line in both the case is close to 1 elucidating that EIS and tafel plot values followed Temkin's adsorption isotherm

3.3. Surface Analysis

3.3.1. X-Ray Diffraction (XRD)

X-ray diffraction was used to determine film formation of the N80 steel in presence and absence of ZSE. The corrosion product over the surface of the N80 steel in 3.5 wt% NaCl solution is shown in figure 5. Peaks at 2θ = 17–18°, 28°, 30°, 36°, 45°, and 68° can be assigned to the oxides of iron. The peaks due to iron appear at 2θ=17–18°, 30°, 45° and 69◦ in presence of ZSE. Thus, it is observed that in absence of inhibitor, the surface of the metal contains iron oxides of iron. The XRD patterns of inhibited surface showed the presence of iron peaks only, the peaks due to oxides of iron are found to be absent [28, 29]. The formation of adsorbed protective film on the surface of metal in the presence of ZSE is clearly reflected from these observations.

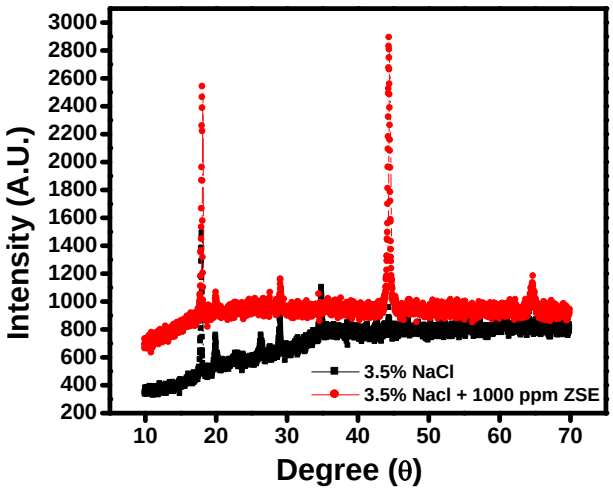

Figure 5. XRD spectrum of N80 steel corrosion in the absence and presence of ZSE.

3.3.2. Scanning Electron Microscopy (SEM)

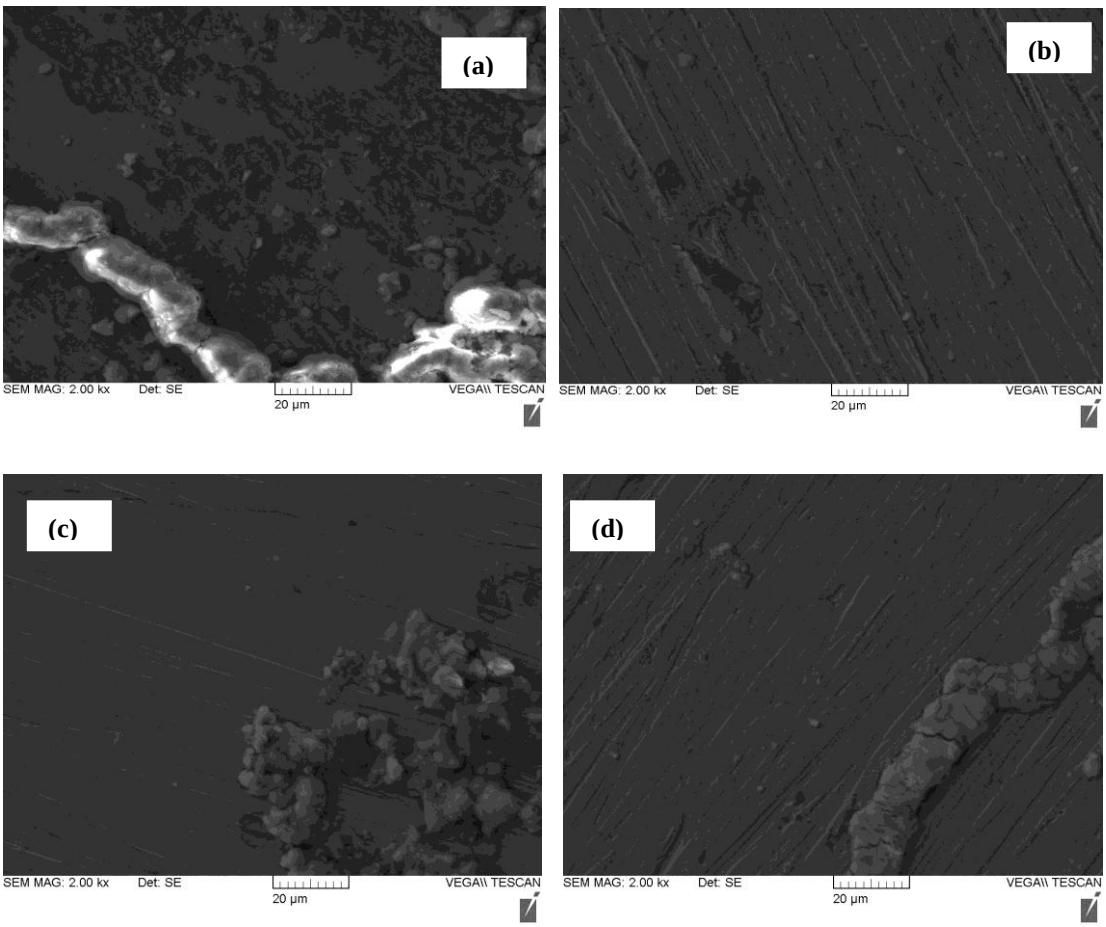

Figure 6. SEM images of N80 steel specimens in (a) 3.5% NaCl (b) 250 ppm ZSE (c) 500 ppm ZSE and (d) 1000 ppm ZSE.

Scanning electron microscopy photographs were taken to show the corrosion inhibition is due to the formation of an adsorptive film on the steel surface. The morphology of the specimen surface in figure 6a showed a corroded surface in the absence of inhibitors, there are pits and cracks on the specimen's surface, and the surface is strongly damaged. However, in the presence of ZSE, the surface corrosion of N80 steel is remarkably decreased. The surface was less corroded and smooth for 250 ppm, 500 ppm and 1000 ppm of ZSE as shown in figure 6b, 6c and 6d. Therefore, a smooth and less corroded morphology of N80 steel samples result from exposure to the inhibitor solutions. These results prove that the ZSE formed a protective film on the metal surface and can effectively protect N80 steel samples from a corrosive environment [30, 31].

4. CONCLUSIONS

In this study, corrosion inhibition efficiency of ZSE on N80 steel in 3.5% NaCl was determined by electrochemical and surface analysis. The potentiodynamic polarization data indicated that the ZSE is mixed type inhibitor. Electrochemical impedance spectroscopy data reveals increase in R_{ct} values which accounted for good inhibition efficiency. The adsorption of the inhibitor molecules on the N80 steel surface was found to obey the Temkin adsorption isotherm for both EIS and tafel. The XRD study confirmed the blockage of metal surface through adsorption process.

ACKNOWLEDGEMENTS
Authors are thankful to the post doctoral fellowship, financial assistance provided by the National Natural Science Foundation of China (No. 51274170) and the research grants from the Colonel Technology Fund of Southwest Petroleum University (Project No.2012XJZ013).

References

1. Mahendra Yadav, Usha Sharma, Premanand Yadav, *Int. J. Ind. Chem.* 4 (2013) 6.
2. D. G. Li, Y. R. Feng, Z. Q. Bai, M. S. Zheng, *Appl. Surf. Sci.* 253 (2007) 8371.
3. Ambrish Singh, M. A. Quraishi, *Res. Chem. Interm.* (2013), http://doi.dx. 10.1007/s11164-013-1398-3.
4. Ambrish Singh, I. Ahamad, M. A. Quraishi, *Arab. J. Chem.* (2012) http://doi.dx.10.1016/j.arabjc.2012.04.029.
5. P. B. Raja, M. Fadaeinasab, A. K. Qureshi, A. A. Rahim, H. Osman, M. Litaudon, K. Awang, *Ind. Eng. Chem. Res.* 52 (2013) 10582.
6. A. Khamis, M. M. Saleh, M. I. Awad, *Corros. Sci.* 66 (2013) 343.
7. Y. Abboud, B. Hammouti, A. Abourriche, A. Bennamara, H. Hannache, *Res. Chem. Intermed.* 38 (2012) 1591.
8. K.R. Ansari, M.A. Quraishi, Ambrish Singh, *Corros. Sci.* 79 (2014) 5.
9. Z. L Liu, S. S. Chu, G. H. Jiang, *J. Agric. Food Chem.* 57 (2009) 10130.
10. V. Iseli, O. Potterat, L. Hagmann, J. Egli, M. Hamburger, *Pharmaz.* 62 (2007) 396.
11. X. G. Yang, *J. Agric. Food Chem.* 56 (2008) 1689.
12. L. Jia, Z. Zhao, S. Lei, Z. Tan, *Food Machin.* 24 (2008) 105.

13. M. A. Quraishi, A. Singh, V. K. Singh, D. K. Yadav, A.K. Singh, *Mater. Chem Phys.* 122(2010) 114.
14. Ambrish Singh, I. Ahamad, V. K. Singh, M. A. Quraishi, *J. Solid State Electr.* 15 (2011) 1087.
15. G. Ji, S. K. Shukla, P. Dwivedi, S. Sundaram, R. Prakash, *Ind. Eng. Chem. Res.* 50 (2011) 11954.
16. Husnu Gerengi, Halil Ibrahim Sahin, *Ind. Eng. Chem. Res.* 51 (2012) 780.
17. S. Sharma, S. Tandon, B. Semwal, K. Singh, *J. Pharm. Res. Opin.* 1 (2011) 42.
18. I. Ahamad, R. Prasad, M. A. Quraishi, *J. Solid State Electrochem.* 14 (2010) 2095.
19. Ambrish Singh, I. Ahamad, V. K. Singh, M. A. Quraishi, *Chem. Engg. Comm.* 199 (2012) 63.
20. N. O. Eddy, S. R. Stoyanov, Eno E. Ebenso, *Int. J. Electrochem. Sci.* 5 (2010) 1127.
21. M. Lebrini, F. Robert, A. Lecante, C. Roos, *Corros. Sci.* 53 (2011) 687.
22. A. Singh, V. K. Singh, M. A. Quraishi, *Int. J. Corros.* doi:10.1155/2010/275983.
23. D. K. Yadav, M. A. Quraishi, B. Maiti, *Corros. Sci.* 55 (2011) 254.
24. A. Singh, Y. Lin, W. Liu, D. Kuanhai, J. Pan, B. Huang, C. Ren, D. Zeng, *J. Taiwan Inst. Chem. Eng.* (2014) http://dx.doi.org/10.1016/j.jtice.2014.02.001.
25. Nnabuk O. Eddy, Femi E. Awe, Abdulfatai A. Siaka, Ladan Magaji, Eno E. Ebenso, *Int. J. Electrochem. Sci.* 6 (2011) 4316.
26. K. F. Khaled, *Electrochim. Acta* 55 (2010) 5375.
27. S. Deng, X. Li, *Corros. Sci.* 55 (2012) 407.
28. P.B. Raja, A.A. Rahim, H. Osman, K. Awang, *Int. J. Miner. Metall. Mater.* 18 (2011) 413.
29. I. O. M. Bockris, B. Yang, *J. Electrochem. Soc.* 138 (2012) 2237.
30. P. B. Raja, A. K. Qureshi, A. A. Rahim, H. Osman, K. Awang, *Corros. Sci.* 69 (2013) 292.
31. A. Singh, Y. Lin, W. Liu, S. Yu, J. Pan, C. Ren, D. Kuanhai, *J. Ind. Eng. Chem.* (2014) http://dx.doi.org/10.1016/j.jiec.2014.01.033.